Phi meson production cross sections in pion-baryon and baryon-baryon interactions

W. S. Chung[1], G. Q. Li[1,2] and C. M. Ko[1]

[1]*Department of Physics and Cyclotron Institute, Texas A&M University, College Station, Texas 77843, U.S.A.*

[2]*Department of Physics, State University of New York at Stony Brook, Stony Brook, New York 11794, U.S.A.*

Abstract

Phi meson production in pion-baryon and baryon-baryon interactions near the production threshold is studied in a boson-exchange model. Parameters in this model are either taken from the Bonn model for the nucleon-nucleon potential or determined from the measured phi meson decay width and the experimental data for the reactions $\pi^- p \to \phi n$ and $pp \to pp\phi$. The isospin-averaged cross sections for the reactions $\pi N \to \phi N$, $\pi\Delta \to \phi N$, $NN \to NN\phi$, which are needed in transport models to study phi meson production in heavy-ion collisions at subthreshold energies, have been evaluated. For the reactions $N\Delta \to NN\phi$ and $\Delta\Delta \to NN\phi$, which become singular when the exchanged pion is on-shell, the Peierls method is used to calculate their cross sections. We find that the cross section for the reaction $\pi N \to \phi N$ is much larger than the other cross sections.

The production of phi mesons, which are pure $\bar{s}s$ states, in hadronic interactions is usually suppressed due to the Okubo-Zweig-Iizuka (OZI) rule [1]. An enhanced production of phi mesons in ultra-relativistic heavy-ion collisions has thus been suggested as a possible signal for the deconfinement phase transition of hadrons to a quark-gluon plasma [2], where the strangeness production rate has been shown to be order-of-magnitude larger than in a free hadronic gas. However, the phi meson properties might be changed in hot dense matter due to the partial restoration of chiral symmetry. Indeed, studies based on QCD sum rules [3,4], hadronic models including vacuum polarization effects [5], and the hidden gauge theory [6] have all shown that the phi meson mass is reduced in medium. The change of phi meson properties can be studied in dilepton spectra [7] and may also be inferred from the phi meson yield in heavy-ion collisions [8].

Phi meson production from heavy-ion collisions has been studied in CERN experiments from the dimuon invariant mass spectra [9]. It has been found that the ratio for ϕ/ω in S+U collisions at 200 GeV/nucleon is enhanced by about a factor of 3 compared to that from the proton-proton and p-U interactions at the same energy. The enhancement can probably be accounted for by assuming that a quark-gluon plasma has been formed in the collisions. On the other hand, it can also be explained by hadronic scenarios [8,10,11]. In particular, it has been pointed out in Ref. [8] that the reactions $K\Lambda \to \phi N$ and $K\bar{K} \to \phi\rho$ become important if one takes into account the medium effects on hadron masses in hot dense matter.

Phi mesons have also been measured recently in heavy-ion collisions at AGS energies from the invariant mass distribution of kaon-antikaon pairs [12], and their mass and width are found to be consistent with that in free space. This is not surprising as these kaon-antikaon pairs are from the decay of phi mesons at freeze out when their properties are the same as in free space. If a phi meson decays in medium, the resulting kaon and antikaon would interact with nucleons, so their invariant mass is modified and can no longer be used to reconstruct the phi meson.

Phi meson production from heavy-ion collisions at SIS/GSI energies are being studied by the FOPI collaboration also through the K^+K^- invariant mass distribution [13]. Their

preliminary results indicate that the ϕ/K^- ratio is about 10%, and is thus similar to that observed at AGS energies. This is quite surprising as the incident energies at GSI and AGS differ by order of magnitude. In a previous study by us [14], the phi meson yield in central Ni+Ni collisions at 2 GeV/nucleon has been studied via its decay into dileptons. Including phi meson production only from the kaon-antikaon annihilation channel, the ϕ/K^- ratio was found to be about 1%, which is much below the value of 10% from the preliminary data of the FOPI collaboration [13]. It is thus necessary to also consider phi meson production from other processes, such as the baryon-baryon and pion-baryon interactions.

There are a number of advantages to work at heavy-ion collisions at SIS energies, which are below the threshold for strange particle production from nucleon-nucleon interactions in free space. First, it has been shown that subthreshold particle production in heavy ion collisions is sensitive to medium modifications of hadron properties [15–17]. Second, at these energies the reaction dynamics is relatively simple as the colliding system consists mainly of nucleons, delta resonances, and pions. In addition to kaon-antikaon annihilation as considered in Ref. [14], phi mesons can be produced from the pion-nucleon, pion-delta, nucleon-nucleon, nucleon-delta, and delta-delta collisions. The cross sections for these reactions are thus needed as inputs in the transport model. Unfortunately, these cross sections are not known empirically near the threshold, which are relevant for phi meson production in heavy ion collisions at subthreshold energies. In this letter, we shall introduce a boson-exchange model to calculate these cross sections. Similar models have been used previously to study pion [18], kaon [19–21], eta meson [22], and dilepton [23] production in nucleon-nucleon interactions in the same energy region.

Specifically, we shall calculate the following cross sections: $\pi N \to N\phi$, $\pi\Delta \to N\phi$, $NN \to NN\phi$, $N\Delta \to NN\phi$, and $\Delta\Delta \to NN\phi$. In principle, one needs for heavy ion collisions the inclusive cross sections such as $NN \to \phi X$ instead of the exclusive cross sections such as $NN \to NN\phi$. Since the energies at SIS are below the phi meson production threshold in the nucleon-nucleon interaction, we expect that exclusive reactions such as $NN \to NN\phi$, which have lower thresholds, are more important than the ones with pions also in the final

state, which require additional energies and are thus suppressed. We note that the boson-exchange model can be generalized to the case with one or two pions in the final state using the approximation of resonance dominance, namely, replacing one or both nucleons in the final state by the delta resonance. Such studies will be pursued in the future.

The Feynman diagrams for $\pi N \to N\phi$ and $\pi\Delta \to N\phi$ are shown in Fig. 1, while those for $NN \to NN\phi$,$N\Delta \to NN\phi$, and $\Delta\Delta \to NN\phi$ are shown in Fig. 2, Fig. 3, and Fig. 4, respectively. For baryon-baryon interactions there is also the exchange diagram as the final nucleons are identical. The Lagrangians for πNN, ρNN, $\rho N\Delta$ [24], and $\pi\rho\phi$ [25] interactions are well-known, and they are given by

$$\mathcal{L}_{\pi NN} = -\frac{f_{\pi NN}}{m_\pi}\bar{\psi}\gamma^5\gamma^\mu\vec{\tau}\psi \cdot \partial_\mu\vec{\pi}, \tag{1}$$

$$\mathcal{L}_{\rho NN} = -g_{\rho NN}\bar{\psi}\gamma^\mu\vec{\tau}\psi \cdot \vec{\rho}_\mu - \frac{f_{\rho NN}}{4m_N}\bar{\psi}\sigma^{\mu\nu}\vec{\tau}\psi \cdot (\partial_\mu\vec{\rho}_\nu - \partial_\nu\vec{\rho}_\mu), \tag{2}$$

$$\mathcal{L}_{\rho N\Delta} = i\frac{f_{\rho N\Delta}}{m_\rho}\bar{\psi}\gamma^5\gamma^\mu\vec{\boldsymbol{T}}\psi^\nu \cdot (\partial_\mu\vec{\rho}_\nu - \partial_\nu\vec{\rho}_\mu) + h.c., \tag{3}$$

$$\mathcal{L}_{\pi\rho\phi} = \frac{f_{\pi\rho\phi}}{m_\phi}\varepsilon^{\mu\nu\alpha\beta}\partial_\mu\vec{\rho}_\nu\partial_\alpha\phi_\beta \cdot \vec{\pi}. \tag{4}$$

In the above, ψ is the nucleon field with mass m_N; ψ_μ is the Rarita-Schwinger field for the spin-3/2 Δ resonance; and π, ρ_μ, ϕ_μ are meson fields with masses m_π, m_ρ, m_ϕ, respectively. The isospin matrices, Dirac γ-matrices and Levi-Civita tensor are denoted by $\vec{\tau}$, γ^μ and $\varepsilon^{\mu\nu\alpha\beta}$, respectively.

The matrix element for the reaction $\pi N \to N\phi$ includes both the vector and tensor contributions and is given by

$$\begin{aligned} M = &\frac{i g_{\rho NN} f_{\pi\rho\phi}}{m_\phi(t - m_\rho^2)}\Big[\bar{u}(p_f)\gamma^\nu u(p_i)\Big]\varepsilon_{\alpha\beta\gamma\nu}q^\alpha\varepsilon^\beta k^\gamma \\ &- \frac{f_{\rho NN} f_{\pi\rho\phi}}{2m_N m_\phi(t - m_\rho^2)}\Big[\bar{u}(p_f)\sigma^{\rho\nu}k_\rho u(p_i)\Big]\varepsilon_{\alpha\beta\gamma\nu}q^\alpha\varepsilon^\beta k^\gamma. \end{aligned} \tag{5}$$

In the above, u and $\bar{u}$ are Dirac spinors of the initial and final nucleons with momenta p_i and p_f, respectively. The momentum and polarization of the phi meson are denoted by q and $\boldsymbol{\varepsilon}$, respectively, while t is the square of the four-momentum k of the exchanged rho meson.

The differential cross section is then

$$\frac{d\sigma}{dt} = \frac{1}{64\pi s}\frac{1}{|\mathbf{p}_\pi|^2}|M|^2, \tag{6}$$

where $\mathbf{p}_\pi$ and $\sqrt{s}$ are, respectively, the pion three-momentum and the total energy in the center-of-mass frame of the pion-nucleon system. In the above equation, the sum over final spins and average over initial spins are implied. We note that in evaluating $|M|^2$ in the above equation and also that for other reactions discussed below, the program Form (Version 1.0) [26] has been extensively used.

The coupling constants ($f_{\pi NN}$, $g_{\rho NN}$, $f_{\rho NN}$, $f_{\rho N\Delta}$) and cut-off parameters in $\mathcal{L}_{\pi NN}$, $\mathcal{L}_{\rho NN}$, and $\mathcal{L}_{\rho N\Delta}$ are taken from the Bonn one-boson-exchange model (Model II) as listed in Table B.1 of Ref. [24]. From the measured width $\Gamma_{\phi\to\pi\rho} \approx 0.6$ MeV, the coupling constant $f_{\pi\rho\phi} \approx 1.04$ is determined. In addition to the form factor at the ρNN vertex which is taken from the Bonn model, we also introduce a monopole form factor with a cut-off parameter $\Lambda^\rho_{\pi\rho\phi}$ at the $\pi\rho\phi$ vertex. By fitting to the available experimental data for the reaction $\pi^- p \to \phi n$ [27], we obtain $\Lambda^\rho_{\pi\rho\phi} = 1.2$ GeV. The comparison of the calculated cross section (solid curve) with the data (open circles) is shown in Fig. 5. We see that the dominant contribution comes from the tensor ρNN coupling (long-dashed curve) as that from the vector ρNN coupling (short-dashed curve) and the interference term (dot-dashed curve) are small. In the same figure, we also show the parameterization introduced by Sibirtsev [28] (dotted curve). Although both are similar at energies where data exist, they differ appreciably near the threshold.

Having determined the cut-off parameter, we can calculate the isospin-averaged cross sections for $\pi N \to N\phi$ and $\pi\Delta \to N\phi$ without introducing further free parameters. In our study the Δ particle is treated by the usual Rarita-Schwinger formalism, with its spin projection operator given by

$$P^{\mu\nu} = -(\not{P} + m_\Delta)\left(g^{\mu\nu} - \frac{1}{3}\gamma^\mu\gamma^\nu - \frac{2P^\mu P^\nu}{3m_\Delta^2} + \frac{P^\mu\gamma^\nu - P^\nu\gamma^\mu}{3m_\Delta}\right). \tag{7}$$

The results are shown in Fig. 6. We see that the cross section for $\pi N \to N\phi$ (solid curve) is about a factor of five larger than that of $\pi\Delta \to N\phi$ (dotted curve), mainly because of the tensor ρNN coupling in the former reaction.

The matrix element for $NN \to NN\phi$ includes both the direct and exchange terms and is given by

$$M = M_d + M_e, \tag{8}$$

where

$$\begin{aligned} M_d = & -\frac{f_{\pi NN} g_{\rho NN} f_{\pi\rho\phi}}{m_\pi m_\phi (q_{1d}^2 - m_\pi^2)(q_{2d}^2 - m_\rho^2)} \Big[\bar{u}(p_3)\gamma_5 \not{q}_{1d} u(p_1)\Big] \Big[\bar{u}(p_4)\gamma^\beta u(p_2)\Big] \varepsilon_{\mu\nu\alpha\beta} q^\mu \varepsilon_\nu q_{2d}^\alpha \\ & - \frac{i f_{\pi NN} f_{\rho NN} f_{\pi\rho\phi}}{2m_N m_\pi m_\phi (q_{1d}^2 - m_\pi^2)(q_{2d}^2 - m_\rho^2)} \Big[\bar{u}(p_3)\gamma_5 \not{q}_{1d} u(p_1)\Big] \Big[\bar{u}(p_4)\sigma_{\rho\beta} u(p_2)\Big] \\ & \cdot\ \varepsilon^{\mu\nu\alpha\beta} q_\mu \varepsilon_\nu (q_{2d})_\alpha q_{2d}^\rho, \end{aligned} \tag{9}$$

and

$$\begin{aligned} M_e = & -\frac{f_{\pi NN} g_{\rho NN} f_{\pi\rho\phi}}{m_\pi m_\phi (q_{1e}^2 - m_\pi^2)(q_{2e}^2 - m_\rho^2)} \Big[\bar{u}(p_4)\gamma_5 \not{q}_{1e} u(p_1)\Big] \Big[\bar{u}(p_3)\gamma^\beta u(p_2)\Big] \varepsilon_{\mu\nu\alpha\beta} q^\mu \varepsilon_\nu q_{2e}^\alpha \\ & - \frac{i f_{\pi NN} f_{\rho NN} f_{\pi\rho\phi}}{2m_N m_\pi m_\phi (q_{1e}^2 - m_\pi^2)(q_{2e}^2 - m_\rho^2)} \Big[\bar{u}(p_4)\gamma_5 \not{q}_{1e} u(p_1)\Big] \Big[\bar{u}(p_3)\sigma_{\rho\beta} u(p_2)\Big] \\ & \cdot\ \varepsilon^{\mu\nu\alpha\beta} q_\mu \varepsilon_\nu (q_{2e})_\alpha q_{2e}^\rho. \end{aligned} \tag{10}$$

In the above, p_1 and p_2 are the four-momenta of two initial nucleons; p_3 and p_4 are those of final nucleons; and q and ε are, respectively the momentum and polarization of the phi meson. The momenta of the exchanged pion and rho meson are denoted, respectively, by $q_{1d} = p_3 - p_1$ and $q_{2d} = p_4 - p_2$ for the direct term and by $q_{1e} = p_4 - p_1$ and $q_{2e} = p_3 - p_2$ for the exchange term.

For the reaction $NN \to NN\phi$, in addition to the usual form factors at the πNN and ρNN vertices taken from the Bonn potential model, two additional monopole from factors are introduced at the $\pi\rho\phi$ vertex as both pion and rho meson are off-shell. The one associated with the rho meson is taken to be the same as in the reaction $\pi N \to N\phi$. The other one associated with the pion introduces another cut-off parameter $\Lambda^\pi_{\pi\rho\phi}$, and it can be determined by fitting to the cross section for the reaction $pp \to pp\phi$. Unfortunately, no experimental data are available for this reaction near the threshold where the boson-exchange model is expected to be appropriate. Nevertheless, we choose $\Lambda^\pi_{\pi\rho\phi}$=0.95 GeV to fit the experimental

data at $p_{lab} \approx 10$ GeV [29,30], which is the lowest beam energy with experimental data available. The resulting cross section is shown in Fig. 7 by the solid curve together with the experimental data (open circle). It should be noted that $\Lambda^{\rho}_{\pi\rho\phi}$ and $\Lambda^{\pi}_{\pi\rho\phi}$ are both in the order of 1 GeV, similar to typical values for cut-off parameters in the Bonn potential model.

The cross section for $pp \to pp\phi$ has also been studied by Sibirtsev [28] based on an one-pion-exchange model. In this study, both the off-shell feature of the pion and the interference between the direct and exchange diagrams are neglected, and the cross section for $pp \to pp\phi$ can thus be expressed in terms of the $\pi^- p \to \phi n$ cross section, which is taken from the empirically measured one. This approach, first introduced in Ref. [31], has been used earlier for calculating kaon production cross section in the nucleon-nucleon interaction [19,21]. The results of Ref. [28] (dotted curve) are seen to be significantly larger than our results, which includes both the off-shell and interference effects. Experiments on phi meson production from the proton-proton collision near the threshold are being carried out at SATURN [32]. These data will be very useful in checking the validity of our model.

The extension of the model to phi production in nucleon-delta ($N\Delta$) and delta-delta ($\Delta\Delta$) interactions is straightforward, except for the complication arising from the fact that at the $\pi N\Delta$ vertex the energy momentum conservation allows the pion to go on-shell. A pole thus develops in the pion propagator at some region of the phase space, which then leads to a singular cross section. Similar singularities appear also in $N\Delta \to N\Lambda K$ [21] and $N\Delta \to NN\eta$ [22]. In both Ref. [21] and Ref. [22], a complex pion self-energy has been introduced to remove the singularity. Since the pion self-energy is density dependent, the resulting cross section becomes density dependent, and diverges when the density approaches zero. This treatment also introduces certain model dependence as different pion self-energies have been used. In Ref. [22], the pion self-energy is related to the pion-nucleon scattering cross section, while in Ref. [21] it is calculated in a simple Δ-hole model.

In this work, this singularity is removed by using the so-called Peierls method [33], which has also been used very recently in the treatment of the singularity in the reaction $\mu^+\mu^- \to e\bar{\nu}W^+$ associated with the physics of muon collider [34]. The basic idea of the

Peierls method is to introduce a complex four-momentum for the resonance in the initial state to account for its finite lifetime. As a result, the four-momentum of the exchanged particle acquires an imaginary part through the energy momentum conservation. In our case, the pion propagator in $N\Delta\rightarrow NN\phi$ and $\Delta\Delta\rightarrow NN\phi$ is modified as follows:

$$\frac{1}{(p_\Delta - p_N)^2 - m_\pi^2} \longrightarrow \frac{1}{(p_\Delta - p_N)^2 - m_\pi^2 - im_\Delta \frac{(E_\Delta - E_N)}{E_\Delta}\Gamma_\Delta}, \tag{11}$$

where p_N and p_Δ are the four momenta of the final nucleon and the initial delta resonance, respectively; E_N and E_Δ are their energies in the center-of-mass frame; and m_Δ is the delta mass. The singularity at $(p_\Delta - p_N)^2 = m_\pi^2$ is seen being removed by the finite delta width $\Gamma_\Delta \approx 120$ MeV. The resulting cross sections are shown in Fig. 8. Near threshold the $N\Delta\rightarrow NN\phi$ cross section (dashed curve) is about a factor of five larger than that of $NN\rightarrow NN\phi$ (solid curve), while the $\Delta\Delta\rightarrow NN\phi$ cross section (dotted curve) is only slightly larger than the latter.

In summary, we have calculated the phi meson production cross sections in pion-baryon and baryon-baryon interactions based on a boson-exchange model. Most parameters in the model are taken from the Bonn model for the nucleon-nucleon potential. Two additional cut-off parameters are introduced at the $\pi\rho\phi$ vertex, and are determined by fitting to available experimental data. We have calculated the isospin averaged cross sections for $\pi N\rightarrow N\phi$, $\pi\Delta\rightarrow N\phi$, $NN\rightarrow NN\phi$, $N\Delta\rightarrow NN\phi$, and $\Delta\Delta\rightarrow NN\phi$ without introducing any further parameters. It is found that the cross section for $\pi N\rightarrow N\phi$ is much larger than the other cross cross sections for phi meson production. These cross sections will be useful for the transport model study of phi meson production in heavy-ion collisions at SIS energies, and such a study will be reported elsewhere [35]. Also, to study possible medium modifications of the phi meson properties, in particular the reduction of its mass, the measurement of dilepton spectra will be very useful [14,36]. Experimentally this will be carried out by the HADES collaboration for heavy-ion collisions at SIS energies [37]. A detailed transport model study of dilepton production including phi meson production from pion-baryon and baryon-baryon interactions and from other processes is also in progress.

We are grateful to W. Kohn for discussions, R. Machleidt and Z. Huang for communications, and P. Lepage for making available to us the subroutine VEGAS for carrying out the numerical integrations in the calculation of the elementary cross sections. This work was supported in part by the National Science Foundation under Grant No. PHY-9509266. The support of CMK by the Alexander von Humboldt Foundation is also gratefully acknowledged. GQL was also supported in part by the Department of Energy under Grant No. DE-FG02-88ER40388.

REFERENCES

[1] J. F. Donoghue, E. Golowich, and B. R. Holstein, Dynamics of Standard Model, (Cambridge University Press, Cambridge, 1992).

[2] A. Shor, Phys. Rev. Lett. 18 (1985) 1122.

[3] T. Hatsuda and S. H. Lee, Phys. Rev. C 46 (1992) R34.

[4] M. Asakawa and C. M. Ko, Nucl. Phys. A 572 (1994) 732.

[5] H. Kuwaraba and T. Hatsuda, Prog. Theor. Phys. 94 (1995) 1163.

[6] C. S. Song, Phys. Lett. B 388 (1996) 1410.

[7] E. Shuryak and V. Thorsson, Nucl. Phys. A 536 (1992) 739.

[8] C. M. Ko and B. H. Sa, Phys. Lett. B 258 (1991) 6.

[9] J. P. Guilland *et al.*, Nucl. Phys. A 525 (1991) 499c.

[10] M. Berenguer, H. Sorge, and W. Greiner, Phys. Lett. B 332 (1994) 15.

[11] P. Koch, U. Heinz, and J. Pisút, Phys. Lett. B 243 (1990) 149.

[12] Y. Akiba *et al.*,, Phys. Rev. Lett. 76 (1996) 2021.

[13] N. Herrmann for FOPI Collaboration, in: Proc. Quark Matter '96, Nucl. Phys. A610 (1996) 49c.

[14] G. Q. Li and C. M. Ko, Nucl. Phys. A 582 (1995) 731.

[15] W. Cassing, V. Metag, U. Mosel, and K. Niita, Phys. Rep. 188 (1990) 363.

[16] U. Mosel, Ann. Rev. Nucl. Part. Sci. 41 (1991) 29.

[17] C. M. Ko and G. Q. Li, J. of Phys. G 22 (1996) 1673.

[18] A. Engel, R. Shyam, U. Mosel, and A. K. Dutt-Mazumder, Nucl. Phys. A603 (1996) 387.

[19] J. Q. Wu and C. M. Ko, Nucl. Phys. A499 (1989) 810.

[20] J. M. Laget, Phys. Lett. B 259 (1991) 24.

[21] G. Q. Li and C. M. Ko, Nucl. Phys. A594 (1995) 439.

[22] W. Peters, U. Mosel, and A. Engel, Z. Phys. A 353 (1995) 333.

[23] L. A. Winckelmann, H. Sorge, H. Stöcker, and W. Greiner, Phys. Rev. C51 (1995) R9.

[24] R. Machleidt, Adv. Nucl. Phys. 19 (1989) 189.

[25] U.-G. Meissner, Phys. Rep. 161 (1988) 213.

[26] J. A. M. Vermaseren, private communication.

[27] A. Baldini *et al.,* Total cross sections of high energy particles, (Springer-Verlag, Heidelberg, 1988).

[28] A. A. Sibirtsev, Nucl. Phys. A604 (1996) 455.

[29] R. Baldi *et al.,* Phys. Lett. B68 (1977) 38.

[30] V. Blobel *et al.,* Phys. Lett. B59 (1975) 88.

[31] T. Yao, Phys. Rev. 125 (1961) 1048.

[32] W. Kohn, private communication.

[33] R. F. Peierls, Phys. Rev. Lett. 6 (1961) 641.

[34] I. F. Ginzburg, Nucl. Phys. B (Proc. Suppl) 51A (1996) 85.

[35] W. S. Chung, G. Q. Li, and C. M. Ko, Nucl. Phys. A, submitted.

[36] Gy. Wolf, W. Cassing, and U Mosel, Nucl. Phys. A 552 (1993) 549.

[37] W. Koenig, in: Proc. Workshop on dilepton production in relativistic heavy-ion collisions, ed. H. Bokemeyer (GSI, Darmstadt, 1994).

FIGURES

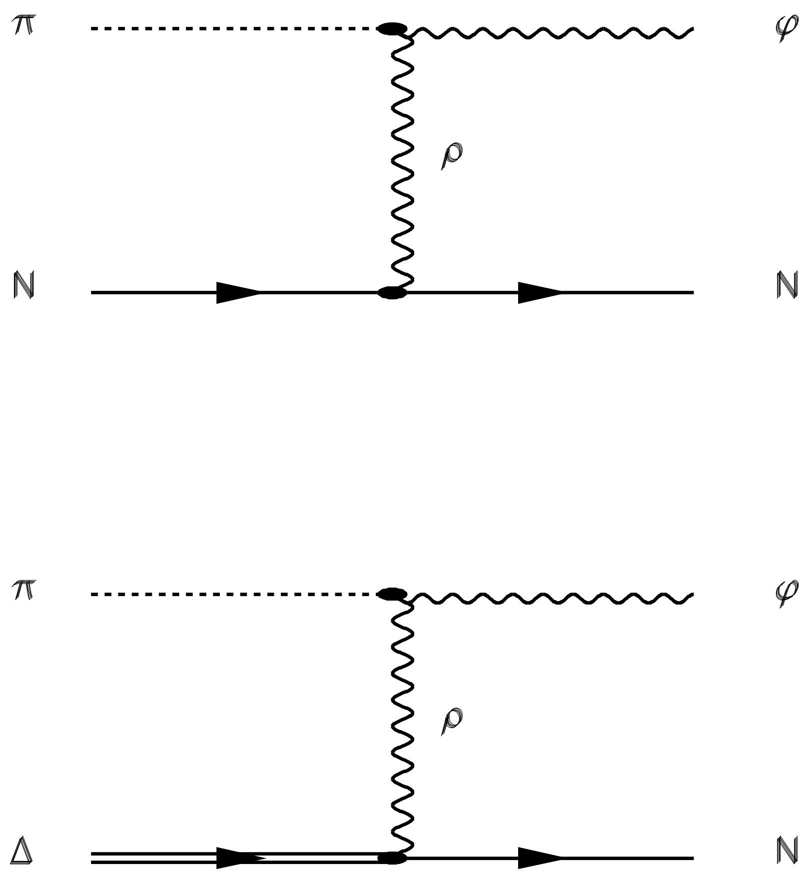

FIG. 1. Feynman diagrams for $\pi N \rightarrow N\phi$ and $\pi\Delta \rightarrow N\phi$.

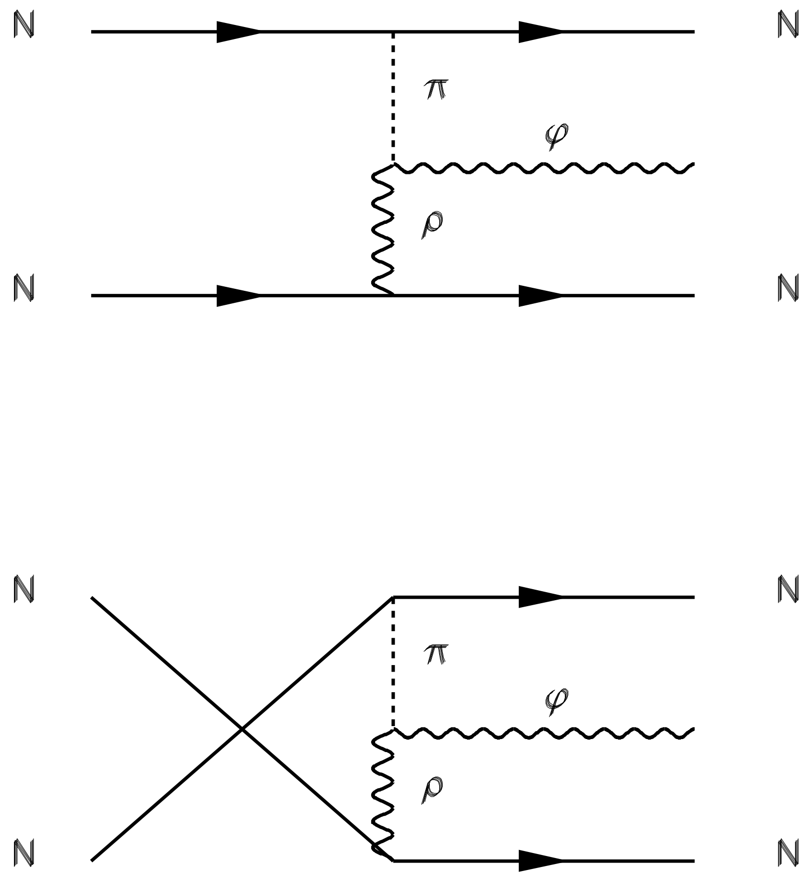

FIG. 2. Feynman diagrams for $NN \rightarrow NN\phi$.

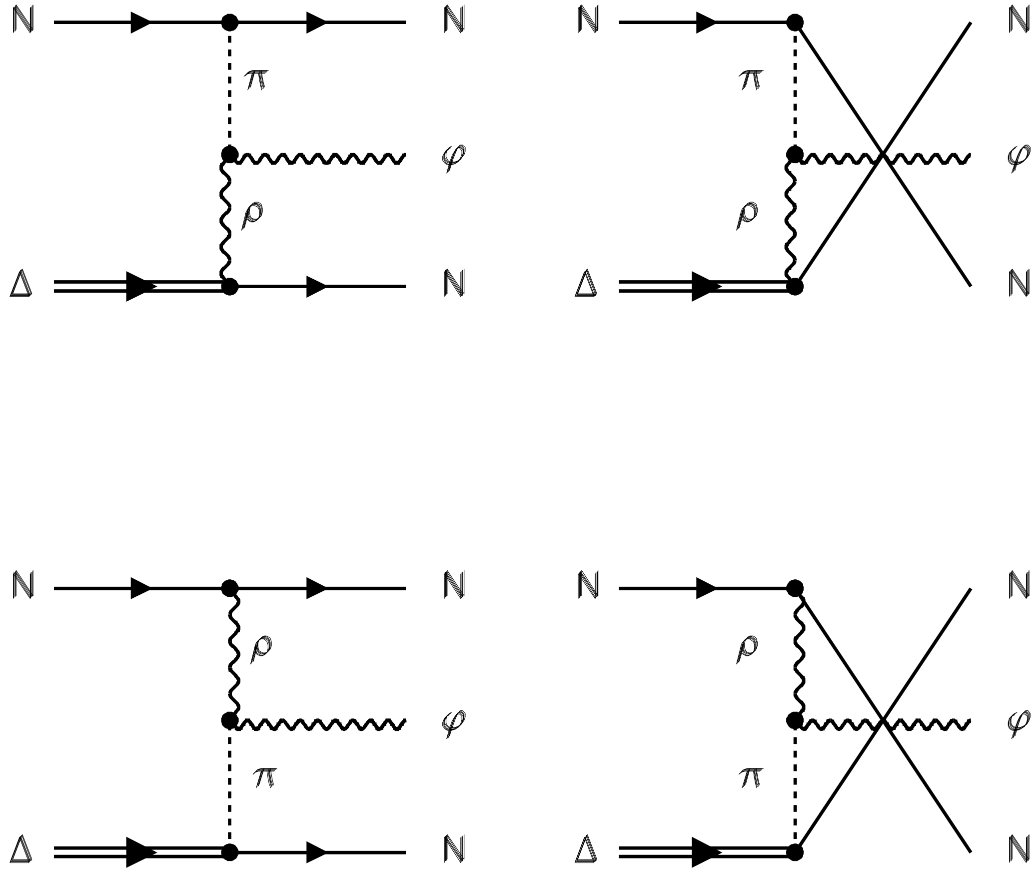

FIG. 3. Feynman diagrams for $N\Delta \rightarrow NN\phi$.

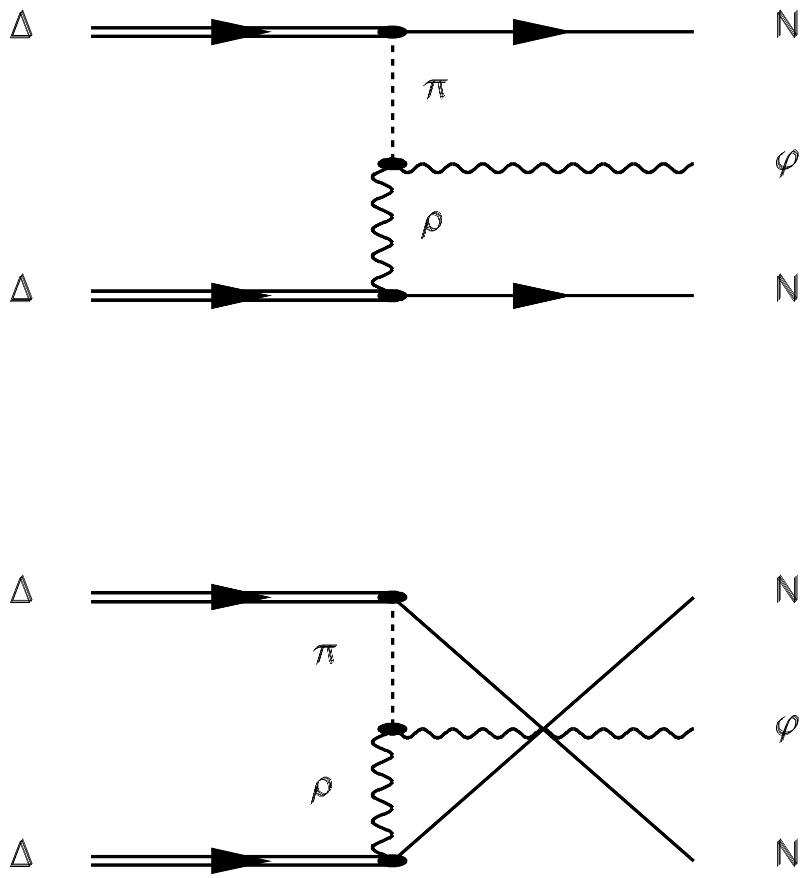

FIG. 4. Feynman diagrams for $\Delta\Delta \rightarrow NN\phi$.

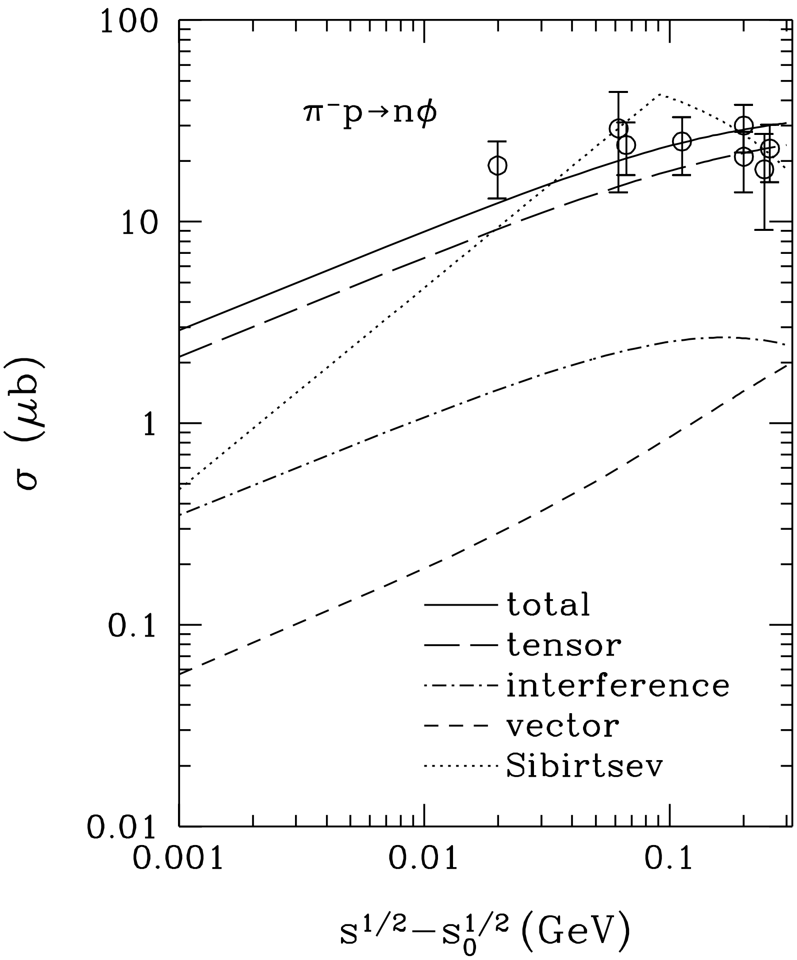

FIG. 5. The cross section for $\pi^- p \to \phi n$.

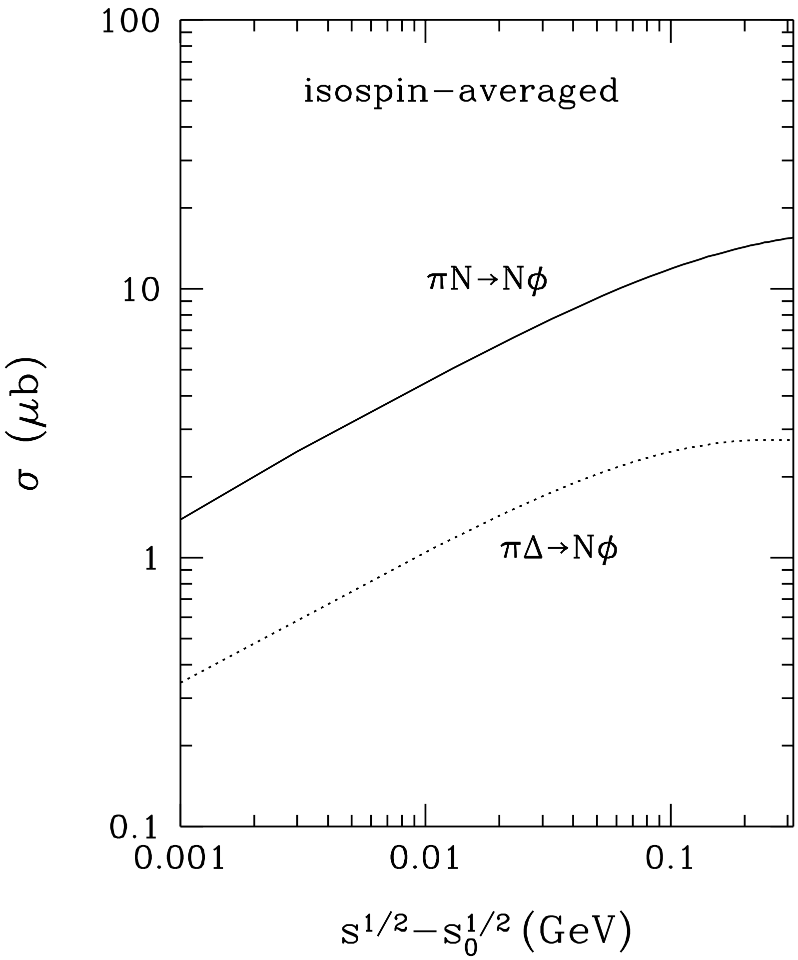

FIG. 6. Isospin-averaged cross sections for $\pi N \to N\phi$ and $\pi\Delta \to N\phi$.

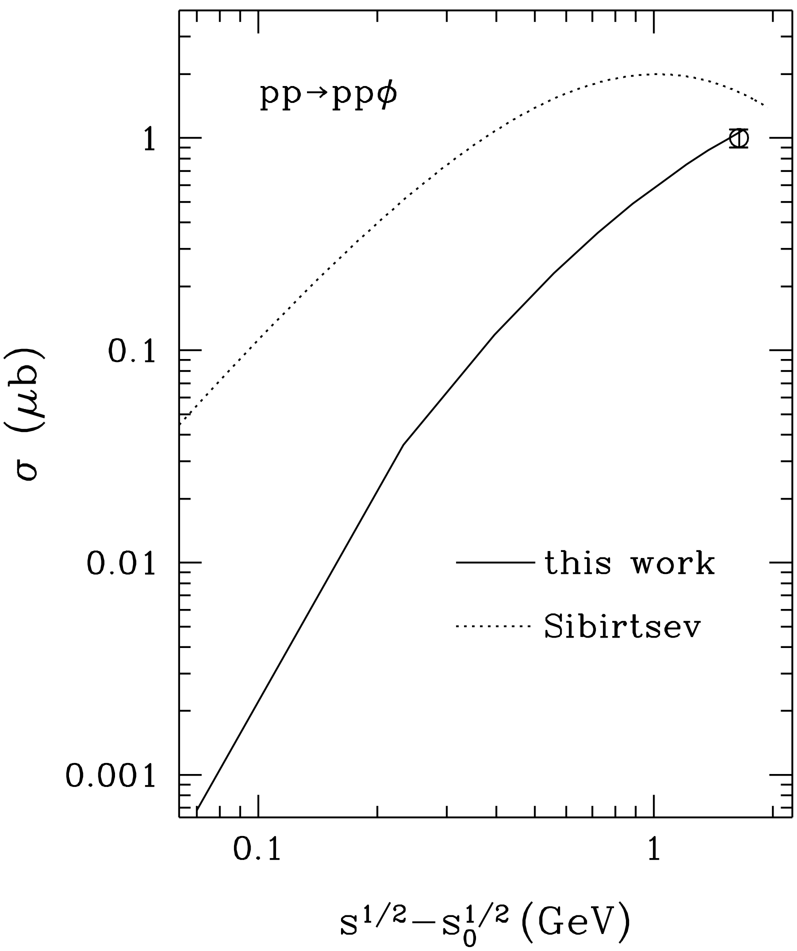

FIG. 7. The cross section for $pp \to pp\phi$.

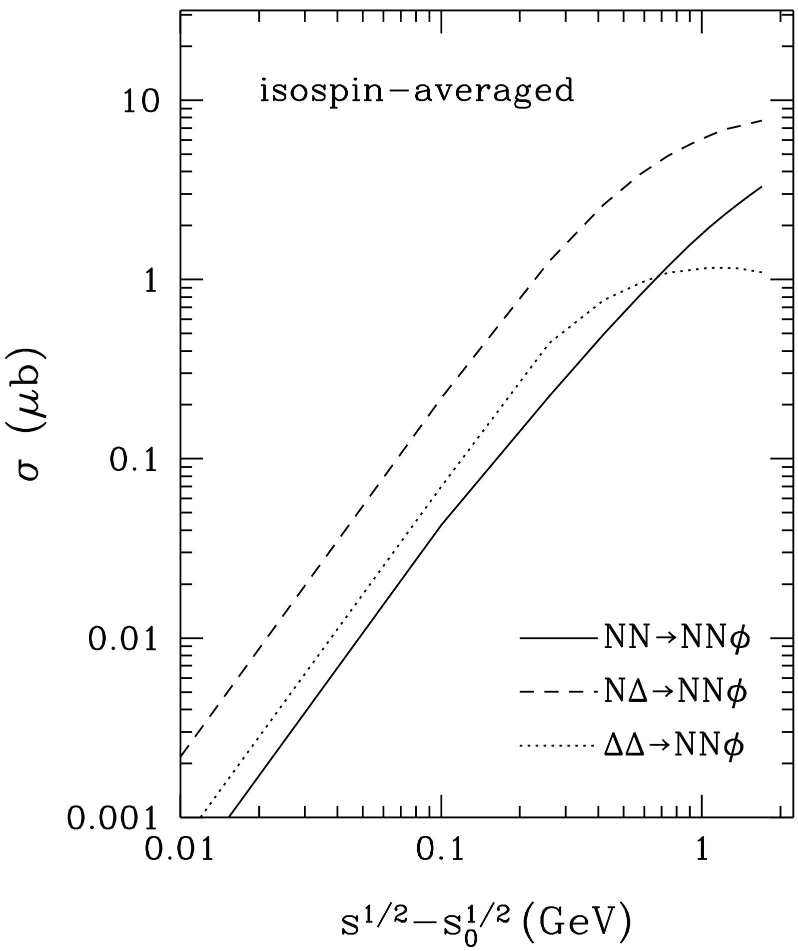

FIG. 8. Isospin-averaged cross sections for $NN\rightarrow NN\phi$, $N\Delta\rightarrow NN\phi$ and $\Delta\Delta\rightarrow NN\phi$.